CIMAC CONGRESS 25
ZURICH, MAY 19 – 23, 2025

2025 | 024

Experimental study of relation between combustion and emission characteristics for ammonia

Visualizations

Shota Hayashida, Oita University

Masaki Tsuda, Oita University
Kohei Shimanouchi, Oita University
Takaya Ishido, Oita University
Hayato Nishimura, Oita University
Kimitoshi Tanoue, Oita University
Kazuyuki Kobayashi, DAIHATSU DIESEL MFG.CO.,LTD
Fuminori Isaka, DAIHATSU DIESEL MFG.CO.,LTD
Asaka Katsuyoshi, Daihatsu Diese MFG.CO.,LTD

ABSTRACT

As countries around the world accelerate their decarbonization efforts to achieve carbon neutrality by 2050, the shipping sector is also moving toward decarbonization. In 2023, the International Maritime Organization (IMO) revised the IMO GHG Reduction Strategy, adopted in 2018, and strengthened its greenhouse gas (GHG) emissions reduction target from international shipping to "zero GHG emissions by around 2050". The "Roadmap Toward Zero Emissions from International Shipping" was formulated in 2020 as a decarbonization initiative in Japan's shipping sector, aiming for commercial operation of "zero-emission ships" that do not emit GHG emissions by 2028, and early commercialization of technologies for highly efficient use of low-carbon alternative fuels is expected. The technology for highly efficient use of low-carbon alternative fuels is expected to be put to practical use as soon as possible. Hydrogen and ammonia, which can be generated from hydrogen, are considered to be promising candidates because they emit no carbon dioxide and are being promoted as a national policy, and there is already a track record of small hydrogen-fueled co-firing ships and fuel cell ships. However, there are some technical issues, such as combustion control, that need to be addressed to accumulate basic research knowledge for early commercialization.

Although there have been many studies on hydrogen and ammonia fuel, few studies have investigated the relationship between combustion characteristics and exhaust gas characteristics when hydrogen and ammonia are co-fired. Ammonia is a flame-retardant fuel that emits a large amount of unburned ammonia, and also generates nitrous oxide (N2O), which has a greenhouse effect 300 times greater than that of carbon dioxide, and fuel-derived nitrogen oxides (fuel NOx). This research aims to solve these problems of ammonia combustion by changing the combustion characteristics by co-firing it with hydrogen, which has high burning velocity. Although there have been previous studies on hydrogen/ammonia co-firing, few studies have systematically investigated the relationship between combustion characteristics and exhaust gas characteristics. This study aims to understand the basic combustion characteristics of hydrogen/ammonia mixed fuel in order to contribute to the development of ammonia/hydrogen co-firing engines for ships to achieve carbon neutrality, which is a national policy. The relationship between combustion characteristics and exhaust gas characteristics will be clarified under various combustion conditions using constant volume chamber and RCEM (Rapid Compression and Expansion Machine).

1 INTRODUCTION

As countries worldwide accelerate their decarbonization efforts, aiming to achieve carbon neutrality by 2050, the shipping sector is also undergoing decarbonization efforts [1]. As part of Japan's efforts to decarbonize its shipping sector, the country aims to achieve the commercial operation of “zero-emission ships” that emit no greenhouse gases by 2028. The early commercialization of technologies for efficiently utilizing low-carbon alternative fuels is also anticipated [2]. Proposed alternative fuels include hydrogen, ammonia, and biofuels. In particular, hydrogen and ammonia, which have zero carbon dioxide emissions, are being promoted as part of national policy. These gases are considered strong candidates based on experience with small-scale hydrogen-fueled co-combustion ships and fuel cell ships. However, several technical challenges remain, requiring further fundamental research for the early practical implementation of this technology.

The direct combustion of ammonia has been attempted in gas turbines [3] and is progressing toward practical application. However, the low burning velocity [4], caused by the flame retardant nature of ammonia, and the high emissions of unburned ammonia remain challenges for practical application. Another major issue is the formation of fuel-derived nitrogen oxides (fuel NO_x) and nitrous oxide (N_2O), which have a greenhouse effect approximately 300 times greater than that of carbon dioxide [5]. Meanwhile, studies have investigated the use of ammonia in reciprocating engines, particularly in compression-ignition engines [6], where its low burning velocity also poses a challenge in spark-ignition engines. To address this issue, similar to gas turbines, research has focused on the co-combustion of ammonia and hydrogen, where hydrogen, with its high burning velocity, is blended with ammonia [7], and stable operation has been reported. However, the emissions of unburned ammonia, nitrogen oxides, and other gases, which are cited as issues in ammonia-only or co-combustion of ammonia and hydrogen, in actual engine exhaust gas data, differ significantly from the results of burners. This may be attributed to heat loss at the wall surface. For example, studies have reported that ammonia emissions in burner experiments are nearly zero on the lean side without heat loss and reach 1000 ppm with heat loss [8]. In contrast, engine experiments show emissions reaching 10,000 ppm, fluctuating down to below 1000 ppm [9] [10]. Similarly, nitrogen oxide emissions exhibit significant differences between engine experimental results and both experimental and numerical analyses of burners.

Based on the above, the emission characteristics observed in engine experiments differ from those in burner experiments It is assumed that the combustion characteristics of spherically propagating flames and the effect of wall quenching have a significant impact on engine experiments. Therefore, when developing models for practical applications, it is necessary to consider both fundamental combustion characteristics, including emission properties, and the effect of wall quenching. However, no research has quantitatively evaluated the effect of wall quenching. Therefore, this study aims to investigate the fundamental combustion characteristics of hydrogen/ammonia fuel blends. Experiments are conducted using a Constant Volume Combustion Chamber (CVCC) and a Rapid Compression and Expansion Machine (RCEM) equipped with a Micro Pilot (MP) injector to clarify the relationship between combustion characteristics and emission characteristics under various combustion conditions.

2 EXPERIMENTAL SETUP

2.1 CVCC (Constant Volume Combustion Chamber)

Figure 1 shows a cross-sectional view and flow path diagram of the CVCC [11] used in this study. The CVCC is a nearly spherical vessel with a total volume of about 13 L. On the top and bottom of the chamber, two fans are installed to perfectly mix the gases. It is also equipped with 150-mm-diameter transparent windows at four sides for flame observation. Central ignition was ignited with the use of an ignition plug, as shown in Fig. 1, with a commercially available automotive spark plug installed at the center of the CVCC.

The experimental process is as follows. First, the fuel and air mixture are made with an arbitrary equivalence ratio by the partial pressure of each component in a premixed gas tank, and the premixed gas is stirred using fans. After sufficient time until the mixture becomes stationary, the combustible mixture is spark-ignited at the center of the chamber. To monitor the pressure and temperature, a pressure gauge and type-K thermocouple were installed on the upper part. Combustion was visualized using the shadowgraph method with a high-speed camera (Phantom VEO 610, acquisition speed: 5000 fps).

In this study, gas composition measurement after combustion was conducted at the same time. Fig.1 shows a flow path diagram of the gas composition measurement. After combustion, the gas to be measured is sampled directly from the exhaust pipe and passed through the heating regulator and capillary. At this time, to prevent the pressure in the

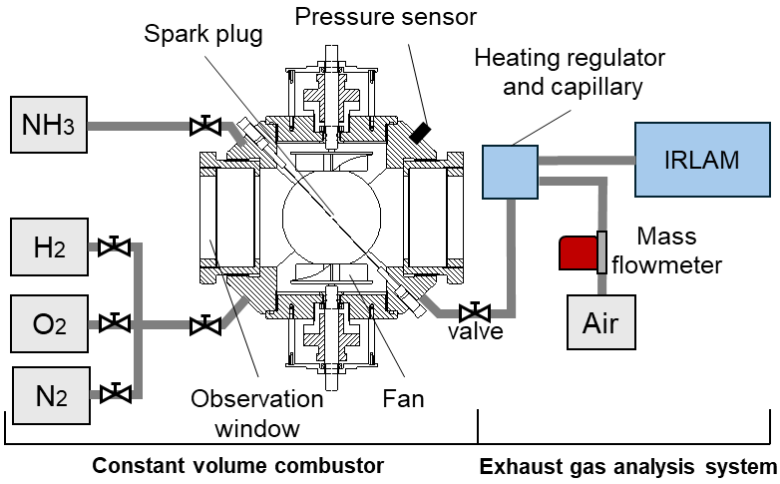

Figure 1. Equipment Schematic (CVCC)

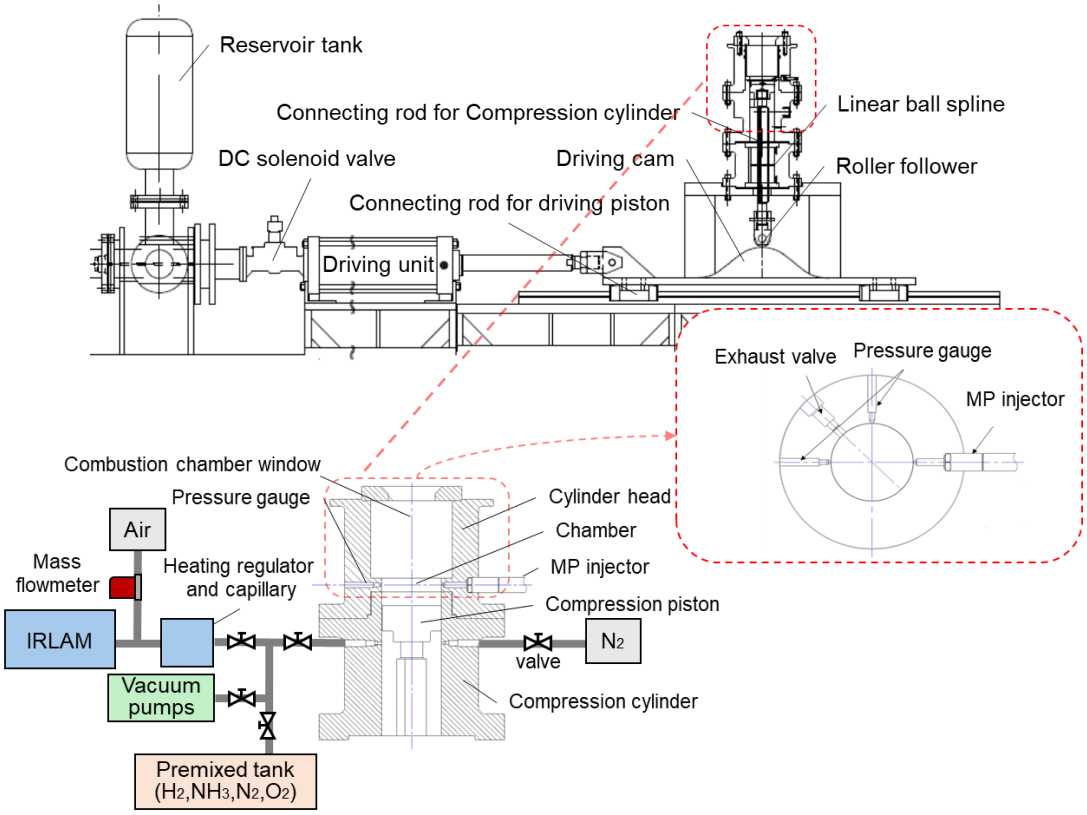

Figure 2. Equipment Schematic (RCEM)

CVCC from dropping, the combustion exhaust gas is pushed out using N_2 gas, and the flow rate through the capillary is maintained at a constant value. The target gas is then diluted with air using a dilution mass flow meter, and the diluted gas flowed into an IRLAM (Infrared Laser Absorption Modulation) analyzer (MEXA-ONE-XL-NX, HORIBA) for measurement. The gas analyzer used in the tests has a measurement range of NO: 200 ppm, NO_2: 100 ppm, N_2O: 200 ppm, and NH_3: 3000 ppm. The measurement accuracy was ±2.0% of the reading, and the zero-point accuracy was NO: ±0.4 ppm, NO_2: ±0.2 ppm, N_2O: ±0.4 ppm, and NH_3: ±6 ppm, respectively.

2.2 RCEM (Rapid Compression and Expansion Machine)

Figure 2 shows a schematic diagram of the RCEM [12] used in this study. The RCEM consists of five elements: a storage section, a drive section, a cam section, a compression section, and a combustion section, and can simulate one cycle of an engine compression and expansion process. The combustion chamber is filled with an ammonia-hydrogen-air mixture and diesel oil is injected and ignited using an MP (Micro Pilot) injector during the compression process. An observation window was installed in

the upper part of the combustion chamber, and an infrared laser (CAVITAR, CABILUX HF) and a high-speed camera (Phantom V 2010, 100,000 fps) were used to observe the jet stream in the main chamber using the shadowgraph method. In addition, the internal pressure in each phase was measured using a pressure sensor (Kistler 6054C) installed in the main chamber. Figure 2 shows a schematic diagram of the measurement of exhaust gas components after the end of combustion. Same as in the CVCC, the gas to be measured was sampled directly from the combustor and passed through a heating regulator and capillary. The combustion exhaust gas was pushed out using N2 gas to prevent the pressure in the combustor from dropping, and the flow rate through the capillary was kept constant. The target gas was then diluted by air supplied from a mass flow meter for dilution and flowed into an IRLAM analyzer for measurement. The same analyzer as CVCC was used, and the components and measurement ranges of the gas analyzer used in the experiments were also identical.

3 EXPERIMENTAL CONDITIONS

The experimental conditions for CVCC and RCEM used in this study are shown in Tables 1 and 2. The mixture composition for each equivalence ratio and the hydrogen addition ratio in the fuel were calculated using the following equations (1) and (2), where δ_{H2} represents the hydrogen addition ratio in the fuel, and X_0 denotes the number of moles of oxygen. The hydrogen addition ratio is the mole fraction.

$$\left(1-\delta_{H_2}\right)NH_3+\left(\delta_{H_2}\right)H_2+X_0(O_2+3.76N_2) \quad (1)$$

$$\phi=\left(3-\delta_{H_2}\right)/4X_0 \quad (2)$$

Table 1. Experimental conditions (CVCC)

Parameter	Conditions
Initial pressure	0.2 [MPa]
Initial temperature	363 [K]
Equivalence ratio Φ	0.65, 0.85, 1.00
Hydrogen addition ratio δ_{H_2}	0, 0.2, 0.4, 0.6 (Φ=0.65 only no ignition for δ_{H_2}=0)

Table 2. Experimental conditions (RCEM)

Parameter	Conditions
Initial pressure	0.2 [MPa]
Initial temperature	373 [K]
Equivalence ratio Φ	0.65, 0.85, 1.00
Hydrogen addition ratio δ_{H_2}	0.2, 0.4, 0.6
Diesel injection timing	-23 [°ATDC]
Bore	80.3 [mm]
Stroke	95 [mm]
Compression ratio	17

4 RESULTS AND DISCUSSION

4.1 CVCC

4.1.1 Flame propagation characteristics

In the experiments using CVCC, visualization experiments were first conducted using the shadowgraph method to investigate the effect of hydrogen addition on laminar flame characteristics.

Figure 3 shows an example of flame images at 14 ms after ignition under the condition of an equivalence ratio Φ of 0.85. From Figure 3, it can be observed that as the hydrogen addition ratio δ_{H2} increases, the spread of the flame becomes faster, and the disturbance of the flame becomes more pronounced.

4.1.2 Laminar flame characteristics

In this study, the laminar burning velocity was calculated from the visualization images as follows. First, the relationship between the flame radius r and elapsed time t was determined from the obtained flame images, and the flame propagation speed, S_b = dr/dt, and the flame stretch rate of the spherical flame, $\kappa = 2/r \times S_b$ were calculated. Then, using the asymptotic analysis of the linear form of the flame stretch, and the flame propagation speed equation derived by Clavin, $S_b = S_b^0 - L_b k$ [13], a least-squares approximation was performed for the "quasi-steady region" [14], excluding the effects of ignition and wall surfaces, to determine the flame propagation speed S_b^0 when there is no stretch. Here, L_b is the Markstein length. From the obtained S_b^0, the laminar burning velocity, S_u^0, was calculated considering the density change as $S_u^0=\rho_b/\rho_u \times S_b^0$.

The relationship between the hydrogen addition ratio δ_{H2} and the laminar burning velocity Su0 is presented in Figures 4 (a), (b), and (c), along with the calculated values using the detailed reaction

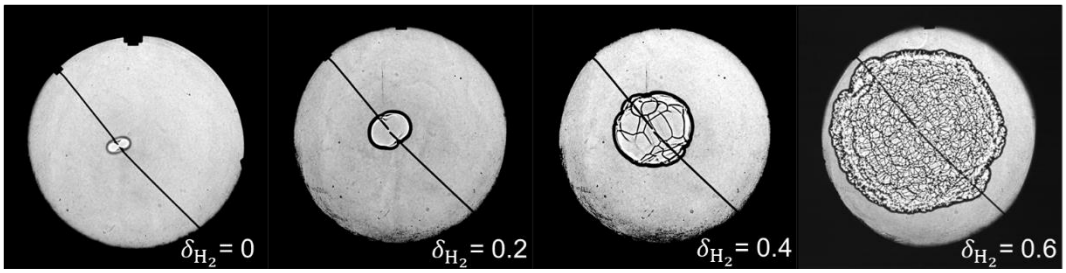

Figure 3. Combustion Visualization (CVCC, Φ=0.85)

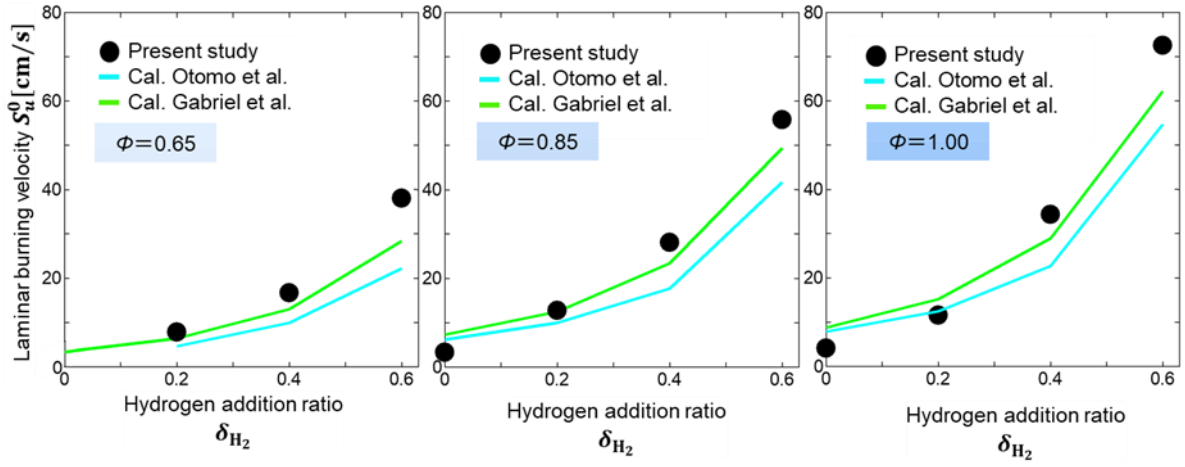

(a) $\phi = 0.65$ (b) $\phi = 0.85$ (C) $\phi = 1.00$

Figure 4. Laminar Burning Velocity Su0 vs. δH2

mechanisms of Otomo et al. [15] and Gotama et al. [16]. The numerical analysis was performed using the chemical reaction analysis software CHEMKIN-PRO [17], and PREMIX was used to calculate the laminar burning velocity. Figure 4 shows that, in all conditions, the numerical analysis results exhibit a similar trend quantitatively.

4.1.3 Emission characteristics of CVCC

Next, in this study, the combustion emission characteristics from the CVCC were investigated. The measurement results of the concentrations of N2O, NO2, and NO in the combustion products from the CVCC are shown in Figure 5(a)(b)(c). The concentrations of N2O, NO2, and NO increased under lean conditions. Moreover, the emissions of NO2 and NO increased as the hydrogen addition ratio δ_{H2} increased under lean conditions, with this trend being particularly prominent at an equivalence ratio Φ of 0.65. This increase in NO2 and NO is attributed to the rise in combustion temperature caused by higher hydrogen addition, which promotes thermal NO_X formation.

The exhaust gas analysis results for NH_3 are shown in Figure 6. From Figure 6, it can be observed that as the equivalence ratio Φ increases, the NH_3 emission concentration also increases, while the emission concentration decreases as the hydrogen addition ratio, δ_{H2}, increases. These results suggest that the concentration of unburned NH_3 in the exhaust gas is correlated with the total amount of NH_3 in the fuel. Therefore, this correlation was examined using the definition formula (3) below.

$$E_{NH_3} = \frac{NH_3\ Emission\ ratio\ [ppm]}{(NH_3\ mole\ fraction)\times 10^6 [ppm]} \quad (3)$$

Figure 7 shows the relationship between the hydrogen addition ratio, δ_{H2}, and the calculated E_{NH3} From Figure 7, it can be observed that as the hydrogen addition ratio δ_{H2} increases, E_{NH3} decreases, suggesting that factors other than the total amount of NH_3 in the fuel are responsible for the reduction in unburned NH_3 concentration. To investigate this factor, the preheat zone thickness, d, which is correlated with the quenching distance [18], was calculated using the following equation (4) to examine the effect of wall quenching.

$$\text{Preheat zone thickness } \boldsymbol{d} = \frac{Thermal\ diffusivity\ \alpha}{Laminar\ burning\ velocity\ S_u^0} \quad (4)$$

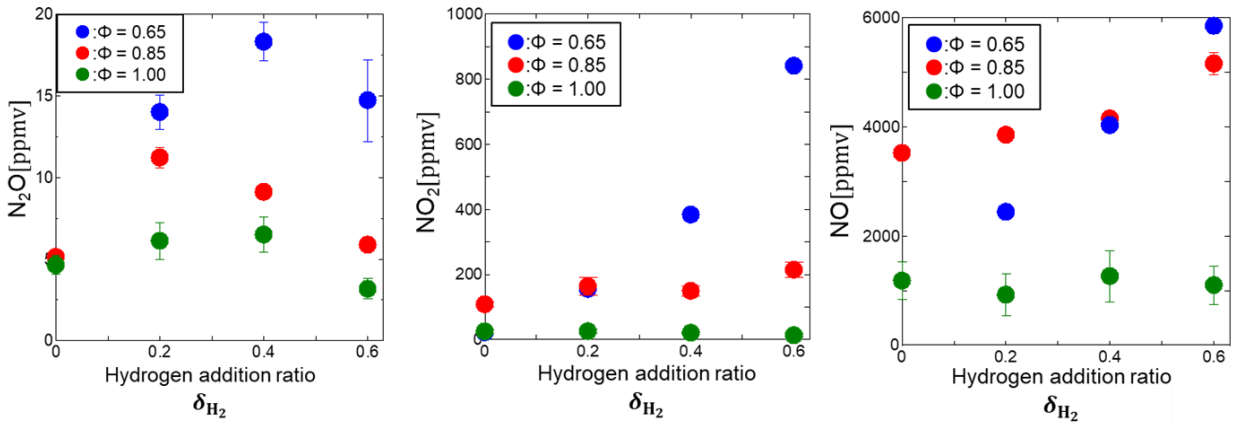

(a) N_2O[ppmv], vs. δH_2 (b) NO_2 [ppmv], vs. δH_2 (c) NO [ppmv], vs. δH_2

Figure 5. Exhaust Gas vs. δH2 (CVCC)

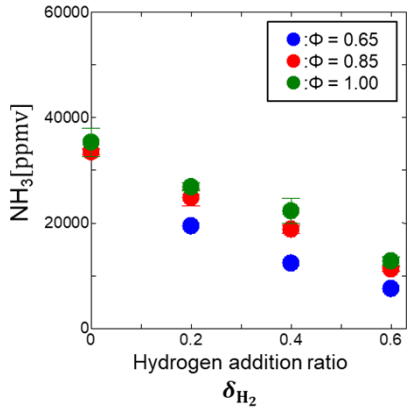

Figure 6. NH_3 [ppmv], vs. δH2

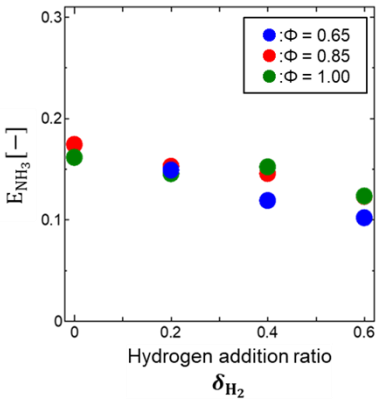

Figure 7. E_{NH3} vs δH2 (CVCC)

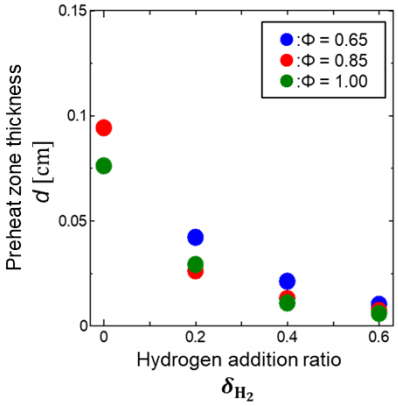

Figure 8. d vs δH2 (CVCC)

Figure 8 shows the relationship between hydrogen addition ratio δ_{H2} and preheat zone thickness, d. From Figure 8, the preheat zone thickness, d, decreases with increasing hydrogen addition ratio, δ_{H2}. Based on these results, the decrease in unburned NH_3 concentration with increasing hydrogen addition ratio δ_{H2} is attributed to the reduction in quenching distance, indicating that the effect of wall quenching is significant.

4.2 RCEM

4.2.1 Flame propagation characteristics

In the experiments using RCEM, the combustion process was also visualized using the shadowgraph method.

Figure 9 shows the flame images after MP injection under the conditions of MP injection timing of -23 [°ATDC], equivalence ratio, 0.85, and hydrogen addition ratios, δ_{H2}, of 0.2 and 0.6. The blue line represents the contour of the diesel fuel, while the red line represents the contour of the flame after ignition. As in the CVCC experiments, it can be observed that as the hydrogen addition ratio, δ_{H2}, increases, the disturbance of the flame front intensifies, and the combustion spread accelerates.

4.2.2 Combustion characteristics

Next, in the experiment using RCEM, the effect of hydrogen addition was examined by analyzing the combustion chamber pressure history under various conditions. Figure 10 (a), (b), and (c) show the combustion chamber pressure histories for each equivalence ratio at the fuel injection timing of -23 [°ATDC] for different hydrogen addition ratios. The blue line represents the result with only diesel fuel. From Figure 10, it can be observed that the pressures of hydrogen-ammonia fuels reach the maximum pressure in the combustion chamber later than in the diesel-only case. This is thought to be due to the relative decrease in oxygen in the combustion chamber. Additionally, the increase in the maximum pressure in the combustion chamber with increasing hydrogen addition ratio δ_{H2} indicates that the burning velocity is enhanced by the addition of hydrogen.

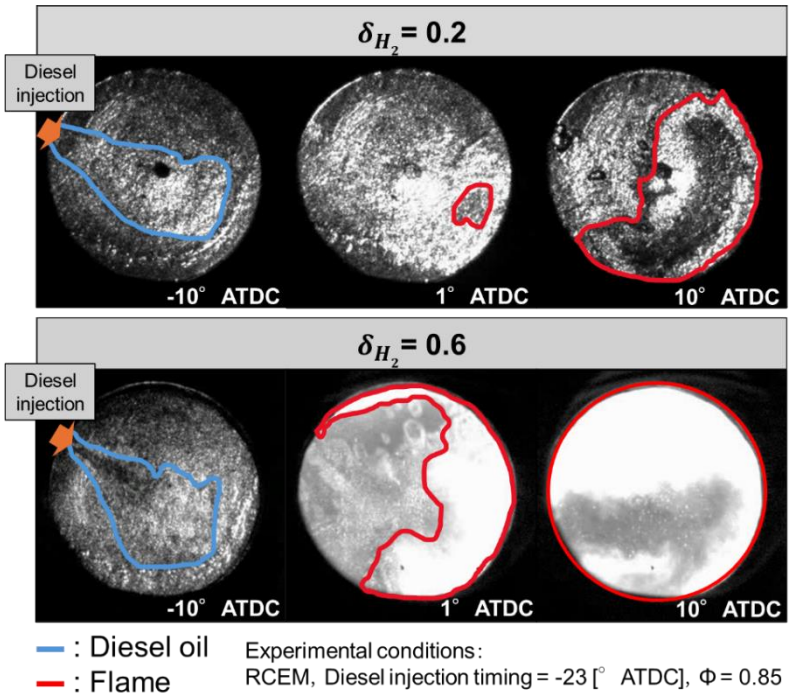

Figure 9. Combustion Visualization (RCEM)

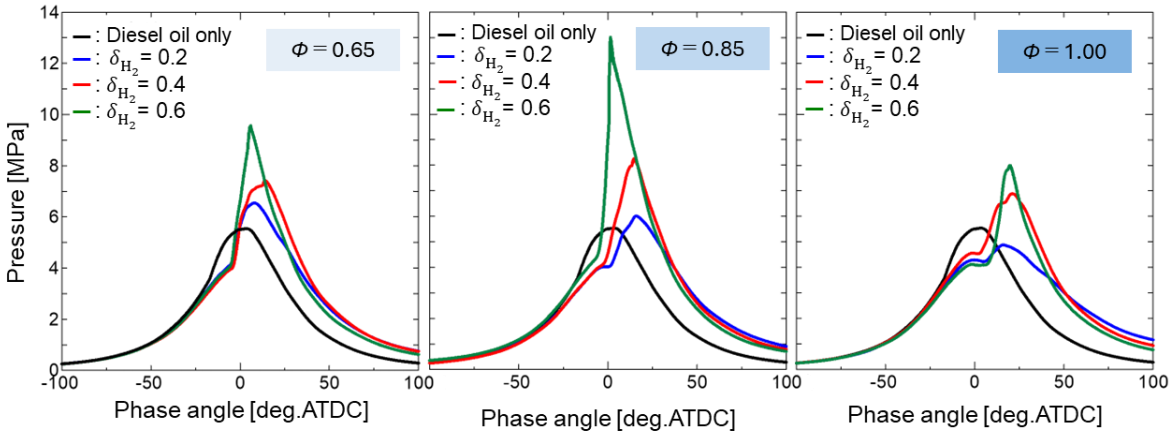

Figure 10. Pressure histories for combustion

4.2.3 Emission characteristics of RCEM

Next, in this study, the combustion emission characteristics from RCEM were investigated. Figure 11 (a), (b), and (c) show the measurement results of N_2O, NO_2, and NO concentrations in the combustion exhaust gases under the condition of diesel injection timing at -23 [°ATDC] using RCEM. From Figure 11, it can be observed that, for all conditions, the results qualitatively follow similar trends to those from CVCC in Figure 5, with a tendency for higher emission concentrations at an equivalence ratio, Φ, of 0.65. Additionally, at an equivalence ratio, Φ, of 0.65, the increase in NO_2 and NO with the increase in hydrogen addition ratio is considered to be due to an increase in thermal NO_X, similar to the findings from CVCC.

On the other hand, comparing Figure 5 and Figure 11 reveals significant quantitative differences. It can be observed that the NO concentration is higher in the CVCC, while the N_2O and NO_2 emission concentrations are higher in the RCEM. These differences may be attributed to variations in combustion conditions (pressure and temperature) and combustion modes (premixed combustion and auto-ignition combustion). A detailed investigation of these factors remains a subject for future study.

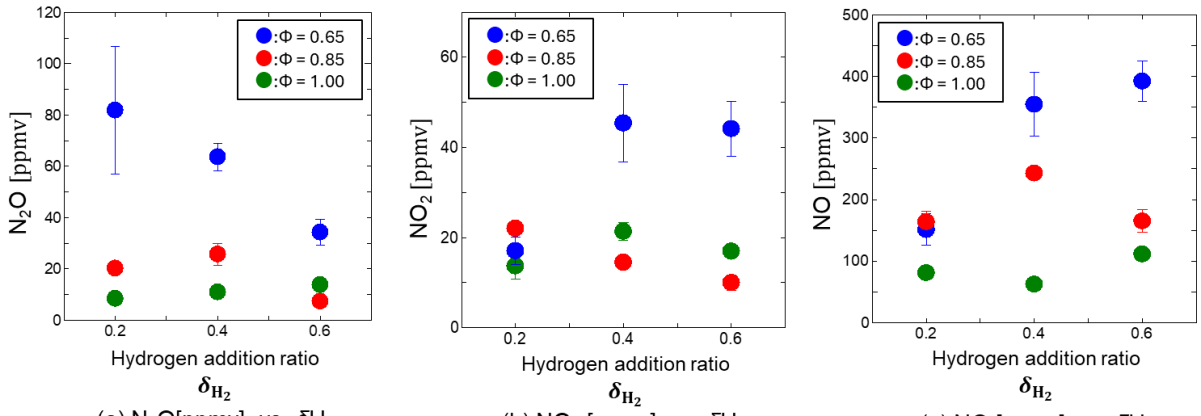

(a) N_2O[ppmv], vs. δH_2 (b) NO_2 [ppmv], vs. δH_2 (c) NO [ppmv], vs. δH_2

Figure 11. Exhaust Gas vs. δ_{H2} (RCEM)

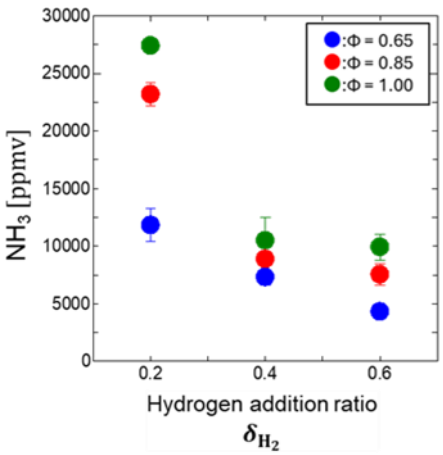

Figure 12. NH_3 [ppmv], vs. δ_{H_2}(RCEM)

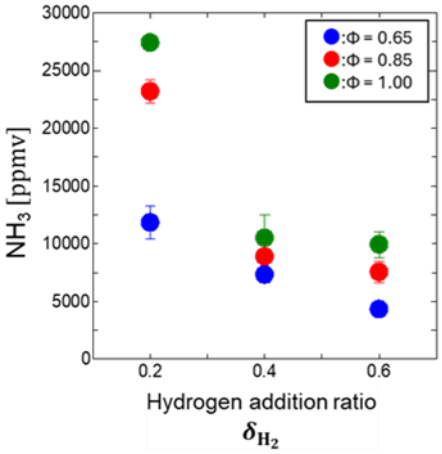

Figure 13. E_{NH_3} vs δ_{H_2}

Figure 12 shows the NH_3 emission concentration in the combustion products. Similar to the emission measurement results using the CVCC, Figure 12 indicates that the NH_3 emission concentration increases as the equivalence ratio, Φ, increases. Additionally, it was observed that the NH_3 emission concentration decreases with an increase in the hydrogen addition ratio, δ_{H2}.Figure 13 shows E_{NH3} calculated using Equation (3). From Figure 13, it can be observed that similar to the experiments using the CVCC, E_{NH3} decreases as the hydrogen addition ratio δ_{H2} increases. This result suggests that the effect of wall quenching is significant.

5 CONCLUSIONS

Through premixed combustion experiments using the CVCC and RCEM, the following conclusions were drawn regarding the fundamental combustion and emission characteristics of the ammonia/hydrogen/Air mixture.

CVCC

1. In the premixed combustion experiments, the laminar burning velocity during hydrogen-ammonia co-combustion was calculated. The experimental results obtained showed a good quantitative agreement with the numerical analysis results.

2. The concentrations of N_2O, NO_2, and NO increased under lean conditions. Additionally, the concentrations of NO_2 and NO increased with the increase in the hydrogen addition ratio on the lean side, and this trend was particularly pronounced at an equivalence ratio of 0.65. This is attributed to the rise in combustion temperature with increasing hydrogen addition ratio, which promotes the formation of NO_2 and NO due to enhanced thermal NO_x production.

3. The NH_3 concentration increased as the equivalence ratio increased, while it decreased as the hydrogen addition ratio increased. The concentration of unburned

NH_3 in the exhaust gases showed a correlation with the total NH_3 content in the fuel, and it was found that the unburned NH_3 emission decreased as the hydrogen addition ratio increased. The decrease in unburned NH_3 concentration with increasing hydrogen addition ratio is attributed to the reduction in flame quenching distance, suggesting that the effect of wall quenching is significant.

RCEM

1. From the visualization images, it was observed that as the hydrogen addition ratio increased, the turbulence of the flame surface became stronger, and the spread of the combustion progressed more rapidly. Additionally, from the pressure history, it was confirmed that the maximum pressure inside the combustion chamber increased with the increase in the hydrogen addition ratio, indicating that hydrogen addition improves the burning velocity.

2. The measurement results of N_2O, NO_2, and NO concentrations qualitatively exhibited a similar trend to the experimental results using the CVCC. However, significant quantitative differences were observed, with higher NO concentrations in the CVCC, while N_2O and NO_2 concentrations were higher in the RCEM. These differences are attributed to variations in combustion conditions, such as pressure and temperature, as well as differences in combustion modes, namely premixed and auto-ignition combustion.

3. The NH_3 concentration measurement results showed that the amount of unburned NH_3 emissions decreased with increasing hydrogen ratio, as in the experiment using CVCC. It is inferred that wall quenching has a significant effect on this factor as well.

6 REFERENCES

[1] Bilgili, L. 2023. A systematic review on the acceptance of alternative marine fuels, *Renewable and Sustainable Energy Reviews* 182: 113367.

[2] Roadmap to Zero Emission from International Shipping, https://www.mlit.go.jp/common/001354313.pdf

[3] Kurata, O., et al. 2017. *Proc. Combust. Inst*. Performances and emission characteristics of NH_3-air and NH_3-CH_4–air combustion gas-turbine power generations, *Proc. Combust. Inst*. 36 (2017) 3351–3359.

[4] Hayakawa, A., et al. 2015. Laminar burning velocity and Markstein length of ammonia/air premixed flames at various pressures, *Fuel*, 159: 98-106.

[5] Kovaleva, M., et al. 2022. Numerical and experimental study of product gas characteristics in premixed ammonia/ methane/ air laminar flames stabilized in a stagnation flow, *Fuel Communications*, 10: 100054.

[6] Reiter AJ., et al. 2008. Demonstration of compression-ignition engine combustion using ammonia in reducing greenhouse gas emissions, *Energy Fuels* 22: 2963-2971.

[7] Frigo, S., et al. 2013. Analysis of the behaviour of a 4-stroke Si engine fuelled with ammonia and hydrogen, *Int. J. Hydrogen Energy*, 38 (3): 1607-1615.

[8] Okafor, E., et al. 2021. Influence of wall heat loss on the emission characteristics of premixed ammonia-air swirling flames interacting with the combustor wall, *Proceedings of the Combustion Institute*, 38 (4): 5139-5146.

[9] Koike, M., et al. 2021. Cold-start performance of an ammonia-fueled spark ignition engine with an on-board fuel reformer, *International Journal of Hydrogen Energy*, 46 (50): 25689-25698.

[10] Qi, Y., et al. 2023. A review on ammonia-hydrogen fueled internal combustion engines, *eTransportation*, 18 : 100288.

[11] Tanoue, K., et al. 2021. Study on the combustion characteristics of furan- and nitromethane-added hydrocarbon fuels, *Fuel*, 287: 119550.

[12] Yamashita R., et al. 2021. Effect of Fuel Property on the Ignition and Combustion Characteristics of Prechamber Ignition, *Journal of Thermal Science and Technology*, 16 (2): p. JTST0014.

[13] Clavin, P. 1985. Dynamic behaviour of premixed flame fronts in laminar and turbulent, flows, *Prog. Energy Combust. Sci*., 11: 1-59.

[14] Kelly, A.P. et al. 2009. Nonlinear effects in the extraction of laminar flame speeds from expanding spherical flames, *Combustion and Flame*, 156 (9): 1844-1851.

[15] Otomo, J., et al. 2018. Chemical kinetic modeling of ammonia oxidation with improved reaction mechanism for ammonia/air and ammonia/ hydrogen/ air combustion, *Int. J. Hydrogen Energy*, 43 (5): 3004-3014

[16] Gotama, G., et al. 2022. Measurement of The Laminar Burning Velocity and Kinetics

Study of The Importance of The Hydrogen Recovery Mechanism of Ammonia/ Hydrogen/ Air Premixed Flames, *Combustion and Flame*, 236: 111753.
[17] ANSYS Chemkin-Pro, ANSYS, Inc., 2022.
[18] Turns, S.R. 2010. *An Introduction to combustion*, McGraw Hill, New York, NY, USA.